Using a titanium-in-quartz geothermometer for crystallization temperature estimation of the Palaeoproterozoic Suursaari quartz porphyry

Kairi Ehrlich[a], Evelin Verš[a], Juho Kirs[b] and Alvar Soesoo[a]

[a] Institute of Geology at Tallinn University of Technology, Ehitajate tee 5, 19086 Tallinn, Estonia; kairi.ehrlich@gmail.com, evelin.versh@kaitseliit.ee, alvar.soesoo@gaia.gi.ee
[b] Institute of Ecology and Earth Sciences, Department of Geology, University of Tartu, Ravila 14a, 50411 Tartu, Estonia; juho.kirs@ut.ee

Received 13 March 2012, accepted 29 October 2012

Abstract. The Suursaari volcanic sequence represents volcanic activity related to Wiborg Batholith rapakivi intrusions in the southern part of the Fennoscandian Shield. The estimated pressure conditions for batholith granitic rocks are 1–5 kbar and crystallization temperatures range from 670 to 890 °C. To describe the temperature regime of the Suursaari volcanic system, a rock sample was taken from the Mäkiinpäällys Mountain outcrop and analysed with laser ablation inductively coupled plasma mass spectrometry. Sample spots were selected from quartz phenocrysts and groundmass. Quartz crystallization temperatures were calculated by the Ti-in-quartz method that takes into account rutile equilibrium and Ti activity in each phase. The calculated crystallization temperatures of the Suursaari quartz porphyry are in the range of 647–738 °C. The results show that the Suursaari quartz porphyry contains two generations of quartz which can be distinguished on the basis of crystallization temperatures: phenocrysts crystallized at higher and groundmass quartz at lower temperature.

Key words: volcanics, quartz porphyry, crystallization temperature, Ti-in-quartz geothermometer, laser ablation inductively coupled plasma mass spectrometry, Suursaari.

INTRODUCTION

Suursaari Island lies in the middle of the Gulf of Finland, approximately 40 km from the coast of Finland and 55 km from the Estonian mainland (Fig. 1). It provides a unique example for studying crystalline basement rocks of the southern margin of the Fennoscandian Shield. Moreover, volcanic products of the Proterozoic rapakivi-type association are well exposed on the island. In fact, Suursaari has yielded the best evidence for volcanic activity associated with the Wiborg batholith (Rämo et al. 2010).

The 1650–1620 Ma rapakivi granites of the Wiborg batholith and its satellites are relatively high-level, epizonal plutons that were emplaced into the ~1.9 Ga Svecofennian crust in an extensional tectonic setting. The current erosional level of the Wiborg batholith corresponds to a palaeodepth of 1–5 kbar (Rämö et al. 2010). Batholith intrusion was associated with a relatively thinned crust, swarms of basaltic and silicic dikes, as well as rare volcanic rocks as those on Suursaari Island. The preserved volcanic sequence on the island is about 200 m thick.

The oldest rocks on Suursaari are various Svecofennian orogenic migmatized gneisses and amphibolites (Koistinen et al. 1996). Svecofennian orogenic rocks are covered with Mesoproterozoic sedimentary Hoglandium conglomerates and mafic (plagioclase porphyrite) and felsic (quartz porphyry) volcanic rocks of rapakivi formation (Koistinen et al. 1996).

High-precision isotope dilution–thermal ionization mass spectrometry U–Pb zircon data on the pyroclastic rhyolitic units from Suursaari imply upper intercept crystallization ages of 1633 ± 2 Ma (Rämö et al. 2010). Epsilon-Nd values of lavas and pyroclastic rocks from Suursaari are slightly negative: around –0.5 for basalts and about –2 for silicic rocks (Rämö et al. 2010). The zircon ages of volcanic products of Suursaari, complying with those of the early and main intrusive phases of the Wiborg rapakivi complex, show that concomitant, quite extensive bimodal volcanism was associated with the emplacement of the Wiborg batholith. It is interesting to note that Estonian rapakivi-type plutons (Soesoo & Niin 1992; Soesoo 1993) fall within the age range similar to that of the Wiborg (U–Pb zircon age 1.650–1.625 Ga; Vaasjoki et al. 1991) varieties: granodiorite of the Märjamaa pluton has yielded a U–Pb zircon age of 1.65–1.63 Ga, Neeme granitoids have given ages of 1.634 and 1.648 Ga and Ereda granitoids 1.642–1.627 Ga (Soesoo et al. 2004; Kirs et al. 2009; Soesoo & Hade 2010).

The age relationships between different units of the Wiborg batholith and associated sequences are well

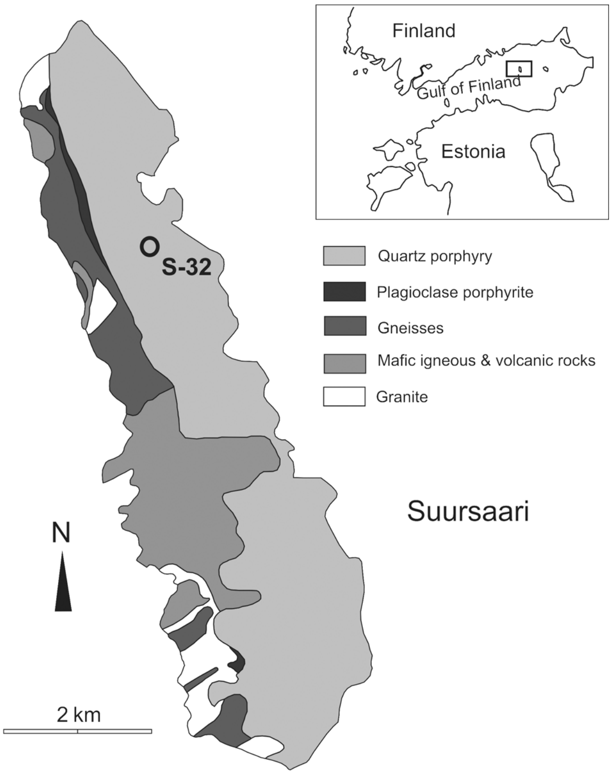

Fig. 1. Geological sketch map of Suursaari (after unpublished materials of H. Koppelmaa, M. Niin and J. Kivisilla, 1970, available in Nironen 2006) and location of sample S-32.

established. However, knowledge on the primary magma emplacement conditions, more specifically temperature and pressure conditions, is still insufficient. Different methods are available to estimate *P–T* conditions, several of which use mineral assemblages or mineral pairs for *P–T* calculations. In order to estimate *P–T* conditions across the entire evolution of a complex magmatic system, single-grain mineral analysis may be helpful, but the number of investigations using single-grain mineral methods is limited. For example, the method estimating the crystallization temperature and pressure based on clinopyroxene composition (e.g. Putirka et al. 1996; Soesoo 1997) cannot be applied to granitic compositions because of the absence of clinopyroxene in the rock.

Recently, a titanium-in-quartz geothermometer (TitaniQ) was developed (Wark & Watson 2006). Due to its novelty and a wide range of applications it has been used in generation temperature research for many rock types. Important applications of the thermometer are the studies on plutonic rocks by Johnson et al. (2009, 2011) and Wiebe et al. (2007), and on volcanic rocks by Wark et al. (2007), Bachmann (2010), Reid et al. (2011), Smith et al. (2010) and Wilcock et al. (2009). Müller et al. (2008) provided an overview of the thermometry of rapakivi granites. Girard & Stix (2010) and Shane et al. (2008) used the thermometer to understand better the magma chamber processes.

The TitaniQ method has been used for hydrothermal (Lowers et al. 2007; Mercer & Reed 2007) and metamorphic rocks (Kohn & Northurp 2009; Spear & Wark 2009; Peterman & Grove 2010; Behr & Platt 2011). The method also provides an opportunity to analyse different quartz zones (Holness & Sawyer 2008; Storm & Spear 2009).

The aim of this paper is to use the titanium-in-quartz thermometer on Suursaari volcanic rocks for refinement of temperature conditions during their formation. Possible applications of the method in the studies of rapakivi-type rocks are assessed.

RAPAKIVI AND RELATED ROCKS – CRYSTALLIZATION TEMPERATURES IN THE MAGMATIC SYSTEM

Temperature and pressure conditions of rapakivi formation have been evaluated on many complexes of the Fennoscandian Shield. The estimated temperatures usually mark the range of 600–900 °C, while pressure conditions for the rock formation range between 1 and 6 kbar (Table 1; Eklund & Shebanov 1999).

An overview of the formation parameters of rapakivi intrusions in the Fennoscandian Shield has been given by Eklund & Shebanov (1999). Temperature conditions between different complexes vary, but usually do not exceed 800 °C, whereas temperatures below 780 °C seem to dominate. There are some exceptions towards higher, up to 850 °C temperatures, especially in granite-related monzonites and granite varieties that are affected by simultaneous mafic magmatism.

Rapakivi granites contain at least two generations of K-feldspar, plagioclase and quartz (Nekvasil 1991; Eklund & Shebanov 1999), although the majority of the reported *P–T* determinations reflect averaged intensive parameters estimated from all generations of major phases in the magmatic system. To give more complete information about this system, it is important to apply thermobarometry directly to different rock/mineral generations (incl. megacrysts, inclusions in megacrysts and groundmass). Eklund & Shebanov (1999) have shown that *P–T* conditions may differ between megacrysts and groundmass. The core zones in feldspar ovoids showed a pressure of about 5–6 kbar and temperature of 680–750 °C, while the cores of quartz megacrysts showed 4.5–6.5 kbar and 720–780 °C, respectively. The matrix of the same rock type gave the values 1–2.5 kbar and 650–750 °C (Eklund & Shebanov 1999).

For example, the two-stage growth of zircon during crystallization of the rapakivi parental magma is consistent

Table 1. Summary of thermometric estimations from the Fennoscandian rapakivi granites

Complex	Rock type	*T*, °C	*P*, kbar	Method	Comments	References
Wiborg (W1)	Wiborgite	670–800	2.5–5.4	Amphibole-plagioclase thermometry	Al in amphibole, amphibole-plagioclase	Elliott 2001
Wiborg (W2)	Wiborgite	710–890	0.7–3.1	Amphibole-plagioclase thermometry	Amphibole in mafic magmatic enclaves and hybrid rocks	Elliott 2001
Wiborg	Wiborgite	650–750	*	Two-feldspar geothermometry	Core of the ovoids	Rämö & Haapala 1995
Wiborg	Wiborgite	580–650	*	Two-feldspar geothermometry	Core of the ovoids	Rämö & Haapala 1995
Salmi	Wiborgite	740–780	*	Zircon thermometry	Early zircon population	Amelin et al. 1997
Salmi	Wiborgite	680–720	*	Zircon thermometry	Late zircon population	Amelin et al. 1997
Uljalegi	Amphibole, quartz phenocryst	700–840/940	*	Zircon crystallization temperature modelling by Watson & Harrison (1983)	Two zircon populations	Amelin et al. 1997
Åland (Å3)	Monzonite	750–840	7.0–8.0	Thermobarometry	Calcic plagioclase with amphibole	Eklund & Shebanov 2005
Åland (Å2)	Monzonite	740–840	6.0–7.0	Thermobarometry	Fe-rich amphibole varieties	Eklund & Shebanov 2005
Åland (Å1)	Monzonite	740–760	4.0–5.0	Thermobarometry	Fe-poor amphibole varieties	Eklund & Shebanov 2005
Åland (Å3)	Rapakivi granite	780–815	*	Crystallization path calculation method	Phenocrysts	Nekvasil 1991
Suursaari	Quartz porphyry	669–726	1.0–1.4	Ti-in-quartz thermobarometry	Quartz phenocrysts	This study
Suursaari	Quartz porphyry	647–738	1.0–1.4	Ti-in-quartz thermobarometry	Quartz in groundmass	This study

* The article provides only temperature data, no pressure conditions are provided.

with the evidence for two distinct mineral assemblages in amphibole-biotite rapakivi granites of the Salmi complex. These were formed in temperature intervals of 740–780 °C and 680–720 °C (Shebanov et al. 1996).

A detailed overview of Wiborg batholith rapakivi crystallization conditions has been given by Elliott (2001). Hornblende-plagioclase thermometry and aluminium-in-hornblende barometry within wiborgite record crystallization temperatures between 670 and 800 °C, at pressures of 2.5–5.4 kbar (Elliott 2001). Amphibole data from mafic magmatic enclaves and hybrid rocks record a wide range of temperatures and pressures between 710 and 890 °C, at pressures of 0.7–3.1 kbar (Elliott 2001).

Väisänen et al. (2000) described *P–T* conditions of post-collisional magmatism in SW Finland. In this region the Palaeoproterozoic mineral assemblages attained equilibrium at average *P–T* values of 4.1 kbar and 680 °C (Väisänen et al. 2000). The post-collisional intrusions intruded at a pressure of at least 4.1 kbar, corresponding to a minimum depth of 14–15 km.

Summarizing the results of mineral crystallization regime investigations on the Fennoscandian rapakivi-type rocks, it is well evident that the rapakivis have formed in polybaric and -thermal conditions (Table 1). In order to gain a better understanding of various stages of the evolutionary sequence, a detailed method is necessary enabling mineral grain-based estimates.

TitaniQ: TITANIUM-IN-QUARTZ GEOTHERMOMETER

Titanium (Ti) is one of many trace elements that substitutes silica (Si) in quartz (Larsen et al. 2000; Flem et al. 2002; Müller et al. 2003a, 2003b; Götze et al. 2004, 2005). A titanium-in-quartz (TitaniQ) geothermometer is based on the idea that Ti concentration in quartz is related to the mineral formation temperature. Higher crystallization temperature means also that Ti concentration in rock is higher (Wark & Watson 2006). In igneous rocks Ti can substitute for Si without having to be charge balanced by coupled substitution of another element, because of the tetravalent nature of both the Ti- and Si-cations (Götze et al. 2001). The activity of Ti in many systems is fixed by the presence of a nearly pure TiO_2 phase (typically rutile, Wark & Watson 2006). Consequently, the chemical potential of Ti, and hence the extent of Ti substitution for Si in quartz, should vary systematically with temperature. The titanium concentration in quartz typically ranges between 1 and 100 ppm, in the quartz of high-temperature rocks the content can be even higher.

The TitaniQ geothermometer is based on the same thermodynamic principles as trace element thermometers Ti-in-zircon and Zr-in-rutile (Wark & Watson 2006). At equilibrium conditions the quartz–rutile exchange reaction can be written as

$$\mathrm{TiO}_2^{\mathrm{rutile}} = \mathrm{TiO}_2^{\mathrm{qtz}}. \quad (1)$$

Wark & Watson (2006) showed experimentally that the Ti concentration in quartz increases exponentially with the reciprocal temperature, and quartz crystallization temperatures, if we do not account for pressure conditions, are calculated by the equation

$$T(°\mathrm{C}) = \frac{-3765}{\log\left(\dfrac{X_{\mathrm{Ti}}^{\mathrm{qtz}}}{\alpha_{\mathrm{TiO_2}}}\right) - 5.69} - 273, \quad (2)$$

where $X_{\mathrm{Ti}}^{\mathrm{qtz}}$ is the Ti concentration in quartz and $\alpha_{\mathrm{TiO_2}}$ is the activity of TiO_2 of the system. In the presence of rutile the $\alpha_{\mathrm{TiO_2}}$ value is ~1 (Wark & Watson 2006). In rocks where Ti concentration is low and mineral rutile has not formed, the $\alpha_{\mathrm{TiO_2}}$ value is <1. In this case the Ti activity must be independently estimated and activity fluctuation by ±0.2 gives an error of ±10 °C in the final calculation (Kohn & Northrup 2009; Spear & Wark 2009).

The advantage of this method is the variable use range, because almost every rock contains quartz that is stable in different pressure and temperature conditions. The TitaniQ geothermometer is especially useful for analysing rocks that crystallized at temperatures above 500 °C.

MATERIAL AND METHODS

Quartz porphyry samples were collected in the NW part of Suursaari Island (during the field work in 1987) at the Mäkiinpäällys Mountain outcrop. The samples belong to the Museum of Geology of the University of Tartu. The main minerals in the sample are quartz, perthitic orthoclase, plagioclase with sericite, epidote and chlorite. Accessory minerals are represented by apatite, zoisite, sphene, calcite, fluorite and magnetite.

Before analysing the samples with laser ablation inductively coupled plasma mass spectrometry (LA-ICP-MS), they were studied with a petrographic microscope and scanning electron microscope (SEM) to determine the possible presence of titanium-containing inclusions and avoid them while analysing quartz. The in-house SEM instrument Zeiss EVO MA15, equipped with an Oxford INCA energy-dispersive spectrometer, was used.

Quartz phenocrysts in the rock are relatively large and surrounded by grey-brown sub-microscopic groundmass (Fig. 2). The petrographic microscope revealed

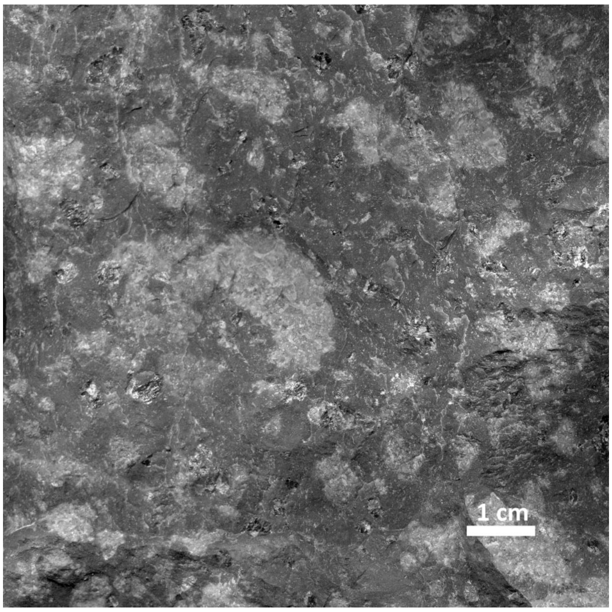

Fig. 2. Suursaari quartz porphyry: quartz and orthoclase phenocrysts (light) in aphanitic groundmass (dark). Sample S-32, Mäkiinpäällys.

in places embayments of the groundmass inside quartz crystals (Fig. 3). To clarify for further examination whether the quartz crystals contain impurities, the samples were studied by SEM. It is extremely important to make sure that the quartz crystals selected for LA-ICP-MS analysis do not contain impurities or inclusions, especially of rutile. The SEM analyses confirm that quartz is pure and has no rutile inclusions (Fig. 4). In some cases, plagioclase, feldspar and accessory magnetite were determined in quartz grains.

Titanium in quartz was measured by using inductively coupled plasma mass spectrometer (a quadrupole X-Series 2 ICP-MS, Thermo Scientific) equipped with the laser ablation system (UP213nm, NewWave).

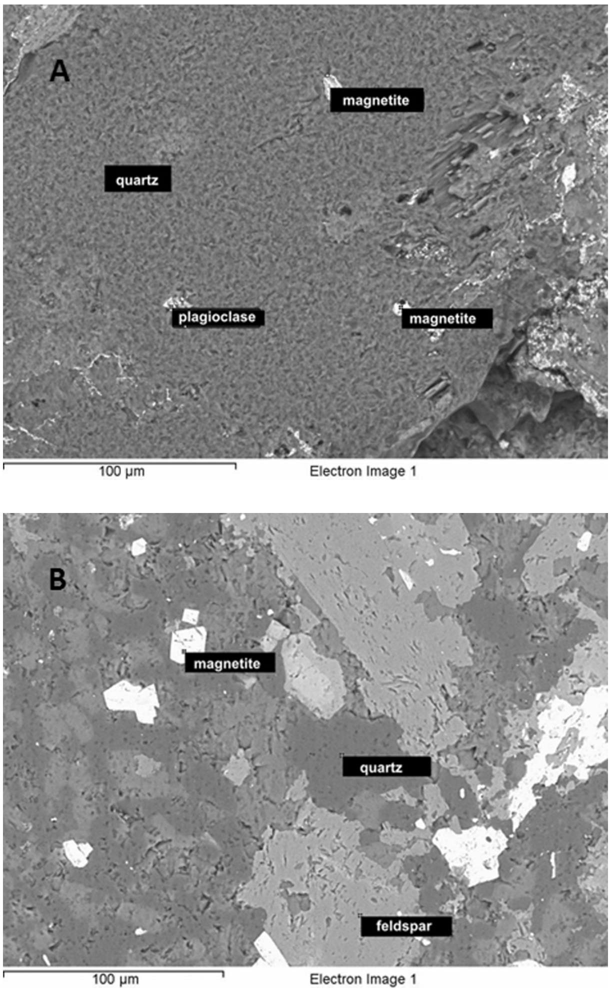

Fig. 4. Suursaari quartz porphyry: magnetite, orthoclase and plagioclase inclusions in quartz phenocryst. Sample S-32, Mäkiinpäällys. Quartz phenocrysts in Suursaari quartz porphyrite contain some accessory minerals: magnetite (**A**, **B**), feldspar (**B**) and plagioclase (**A**). Scanning electron microscope (SEM) images.

A total of 49 spot analyses from porphyritic quartz grains and 40 spot analyses from groundmass in an uncoated thin-section were subjected to LA-ICP-MS analysis. To ablate quartz in both phenocrysts and groundmass, a 40 µm laser beam during 60 s was used. Phenocrysts were ablated on a straight line and a spot was used for groundmass. Before analysing the sample surface was cleaned by ablating it during 1 s. The isotope Si^{29} was used as an internal standard. External calibration was done by using three multi-element silicate glass reference materials produced by the National Institute of Standards and Technology (NIST): SRM 610 (consists of 437 ppm Ti), SRM 612 (50.1 ppm Ti) and SRM 614 (3.1 ppm Ti).

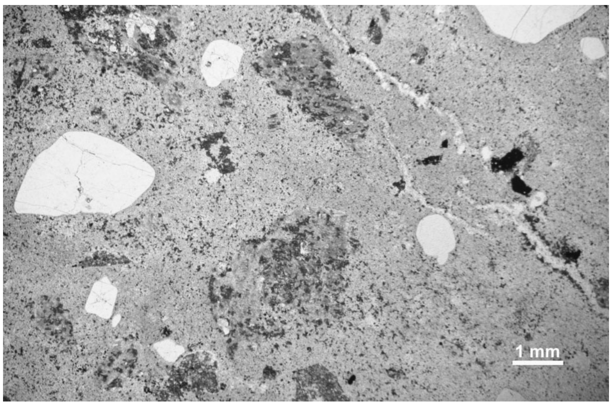

Fig. 3. Suursaari quartz porphyry: quartz and turbid orthoclase phenocrysts in submicroscopic groundmass. Thin-section, backscattered image. Sample S-32, Mäkiinpäällys.

RESULTS AND DISCUSSION

The Ti content of quartz from phenocrysts and groundmass of the Suursaari quartz porphyries together with calculated rock crystallization temperatures are presented in Table 2 and Figs 5 and 6. The average Ti concentration in phenocrysts is approximately 204 ppm and slightly lower in the groundmass, averaging at 187 ppm.

The Ti concentration in phenocrysts ranges between 160.9 and 250.6 ppm (δ± 14.5–26.9). The crystallization

Table 2. Titanium content (measured with laser-ablation ICP-MS) and calculated crystallization temperatures of quartz phenocrysts (49 analyses) and groundmass (40 analyses) in the Suursaari quartz porphyry

Analysis No.	Ti, ppm	δ±	*T*, °C	*T*, °C±
1	208.1	20.2	844	30
2	205.9	20.2	842	30
3	227.3	28.2	856	39
4	212.9	20.3	847	29
5	226.3	20.6	856	28
6	222.7	23.1	853	32
7	248.6	27.7	870	36
8	236.2	21.0	862	28
9	225.4	26.6	855	37
10	179.6	23.8	823	39
11	202.6	21.5	840	32
12	245.5	24.7	868	32
13	203.4	19.7	840	29
14	192.4	14.7	832	23
15	190.0	21.2	831	33
16	242.4	21.8	866	29
17	217.3	21.1	850	30
18	202.1	21.2	839	32
19	183.9	16.8	826	27
20	175.8	17.5	820	29
21	179.9	18.3	823	30
22	194.4	18.3	834	28
23	182.6	18.0	825	29
24	185.3	18.7	827	30
25	191.5	21.0	832	33
26	208.8	19.3	844	28
27	207.4	26.9	843	40
28	206.6	21.7	843	32
29	199.3	16.7	837	25
30	201.0	25.4	839	38
31	172.2	20.5	817	35
32	201.2	17.5	839	26
33	172.9	19.2	818	32
34	186.9	18.0	828	29
35	184.9	18.1	827	29
36	174.2	14.6	819	24
37	160.9	15.7	808	28
38	181.9	20.1	825	33
39	250.6	23.1	871	30
40	192.8	17.9	833	28
41	189.5	20.3	830	32
42	219.9	19.3	852	27
43	203.9	18.3	841	27
44	213.5	26.2	847	38
45	244.3	20.8	867	27
46	210.4	22.7	845	33
47	180.4	14.5	823	24
48	222.0	24.6	853	34
49	218.8	16.8	851	24

Analysis No.	Ti, ppm	δ±	*T*, °C	*T*, °C±
1	151.2	45.2	650	86
2	147.9	24.1	647	46
3	164.6	30.9	662	54
4	161.8	28.2	660	50
5	165.5	28.6	663	50
7	269.9	59.6	738	73
8	183.9	35.0	678	57
9	174.8	34.4	671	58
10	157.9	28.9	656	52
11	163.5	30.6	661	54
12	182.0	36.6	677	60
13	174.5	38.7	670	65
14	254.3	58.9	728	75
16	170.7	29.5	667	50
17	260.4	72.9	732	92
18	167.5	32.6	665	57
19	178.2	36.8	674	61
20	147.9	37.4	647	72
21	157.0	32.0	655	58
22	160.9	35.5	659	64
23	172.9	35.3	669	60
24	179.3	45.9	674	76
25	184.8	41.6	679	67
26	171.0	53.2	667	92
27	186.5	46.3	680	75
28	190.7	46.4	684	74
29	181.1	46.9	676	77
30	183.2	43.5	678	71
31	198.6	46.9	690	72
32	242.9	51.3	721	68
33	190.7	41.3	683	65
34	193.8	51.0	686	80
35	198.5	53.3	689	82
36	209.2	48.2	697	71
37	222.7	47.1	707	66
39	215.3	58.2	702	85
40	197.8	56.0	689	87

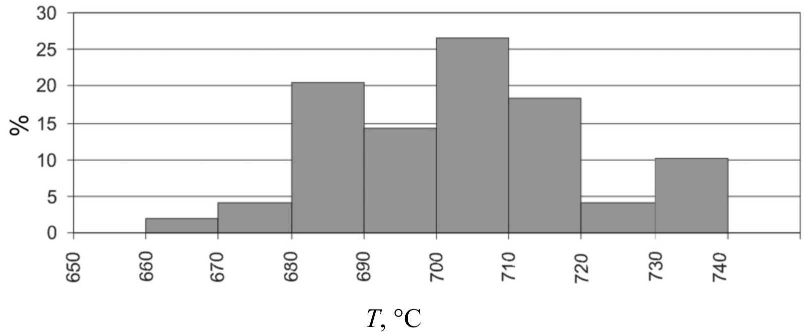

Fig. 5. Percentage distribution of phenocryst quartz crystallization temperatures in the Suursaari quartz porphyry.

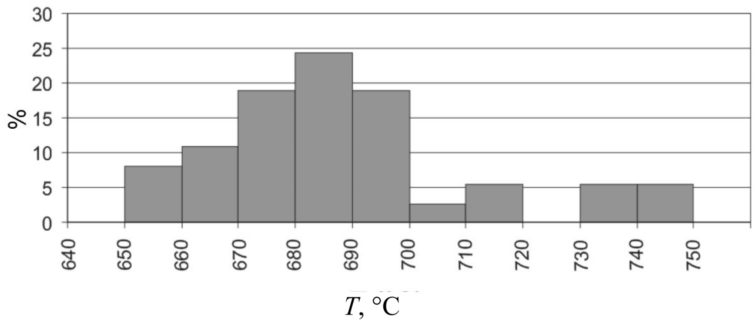

Fig. 6. Percentage distribution of groundmass quartz crystallization temperatures in the Suursaari quartz porphyry.

temperature of the phenocrysts of the Suursaari quartz porphyry calculated according to Eq. (2) and assuming Ti activity of 0.8 varies between 669 and 726 °C (±24 °C) (Table 2). Even though the samples do not contain the rutile phase, the Ti activity of 0.8 is suggested on the basis of the minor presence of apatite and titanomagnetite (as Ti-bearing phases) in the studied samples. The distribution of the measured temperature values of phenocrysts is presented in Fig. 5. The main clustering of the measured values in phenocryst grains falls between 680 and 720 °C, with two temperature peaks around 680 and 700 °C. There may exist a third cluster, pointing towards higher (up to 740 °C) crystallization temperature values.

The measured Ti concentration in groundmass quartz ranges between 147.9 and 269.9 ppm (δ± 24.1–72.9). The calculated quartz crystallization temperatures in groundmass are in the range of 647–738 °C (±50 °C; Table 2).

The obtained data show that quartz in groundmass has generally crystallized at an approximately 20 °C lower temperature than the phenocryst variety. This, indeed, is a logical assumption as groundmass crystallizes later. As seen from Fig. 6, the main range of groundmass quartz crystallization temperature stays within 670–700 °C. The quartz in groundmass shows gradual temperature distribution with the main peak at 680–690 °C. However, the higher-temperature values, up to 750 °C, also exist, which may be derived from early magmatic crystallization processes. This tendency can also be seen in phenocrysts. Some groundmass quartz grains show even higher crystallization temperatures compared to phenocryst quartz. More analyses are needed to understand these relationships.

As shown in Fig. 7, quartz in rapakivi granitic rocks crystallizes mostly at temperatures 700–850 °C, with the tendency towards lower temperature values in lower pressure conditions. The analysed quartz crystallization temperatures from the Suursaari quartz porphyry are close

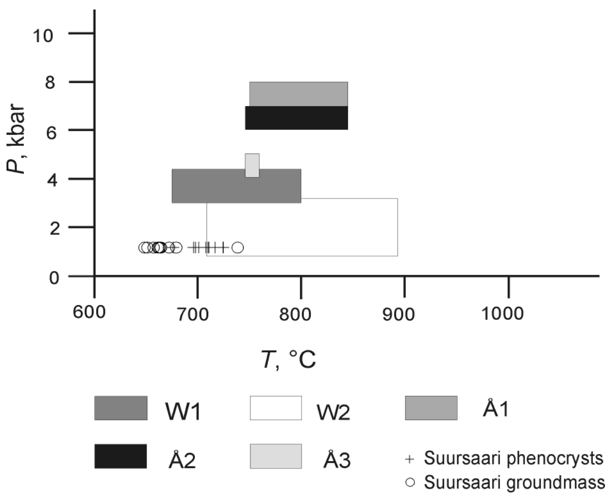

Fig. 7. Suursaari rapakivi intrusion *P–T* conditions in comparison with previously published data on other rapakivi intrusions in the southern slope of the Fennoscandian Shield (for legend references see Table 1).

to the lower values of wiborgite crystallization temperatures from the Wiborg and Salmi plutons (Shebanov et al. 1996; Elliott 2001). According to Elliott (2001), the Wiborg batholith granites emplaced at relatively shallow levels in the crust, with *P–T* values of 0.7–5.4 kbar and 670–890 °C (Table 1). A higher *P–T* crystallization regime (4–8 kbar and 740–840 °C) is characteristic of monzonitic rocks of the Åland batholith (Eklund & Shebanov 2005). However, it should be mentioned that volcanic Suursaari quartz porphyries have undergone intensive hydrothermal alteration (albitization, epidotization, etc.) processes, which may have had some effect on the Ti content in quartz.

In general, quartz varieties in granites, monzonites and diorites that have crystallized at higher temperatures contain more trace elements in its crystal structure than the quartz formed at lower temperature (Larsen et al. 2000). The most widespread trace elements in quartz aside from Ti are Mg, Ca and Cr in natural less-fractioned pegmatites, and Fe, Li and B in more-fractioned pegmatites. Larsen et al. (2004) found Al, P, Li, Ti, Ge and Na in the order of >1 ppm in pegmatitic quartz, whereas K, Fe, Be, B, Ba, Sr and their trace elements were below the detection limit of LA-ICP-MS. Therefore, it is important to study the Suursaari quartz porphyry for all possible trace elements in order to assess the calculated geothermometry data.

This pilot study shows that the TitaniQ geothermometer may give a valuable input into understanding the magmatic history of complex magmatic systems, such as rapakivi formations. A single-crystal-based method is able to distinguish different crystal generations even in a small sample. However, the knowledge about pressure conditions of the magmatic system will greatly expand the understanding of the magmatic history.

Recently, Thomas et al. (2010) studied how pressure influences Ti solubility in quartz. They used the same material (distilled water, TiO_2 and quartz powder (<22 μm) or SiO_2 glass) to synthesize quartz crystals as Wark & Watson (2006). The results of the experiment show that if in the equilibrium phase defined by Eq. (1) the substitution of Ti^{4+} for Si^{4+} is implicit, the site on which Ti resides in the quartz structure is not specified. It is conceivable that Ti may reside on tetrahedral sites or may dissolve into interstitial sites and thermodynamic variables are unique for each solubility mechanism (Thomas et al. 2010). In case the pressure can be constrained to within ±1 kbar, the temperature can be constrained to approximately ±20 °C (Thomas et al. 2010), because the Ti activity increases when pressure decreases. Thus, the method may have important applications in understanding the complex magmatic systems, which have evolved through different pressure and temperature ranges.

CONCLUSIONS

Rapakivi granites are crystallized in polybaric magmatic systems, where pressure and temperature conditions vary between different rapakivi complexes. In a large scale the rock formation temperatures vary in a range of 600–900 °C and pressure conditions are around 1–6 kbar, in some cases even higher. The Suursaari quartz porphyry is a good example of a volcanic rapakivi rock, containing idiomorphic quartz phenocrysts. Analysis of quartz porphyries with LA-ICP-MS using the TitaniQ geothermometer allows measuring each quartz phenocryst and quartz in groundmass separately, thus having an advantage of providing information on various quartz generations. The crystallization temperatures of the Suursaari quartz porphyry phenocrysts range from 669 to 726 °C, and those of the groundmass vary between 647 and 738 °C. The analysed quartz crystallization temperatures are close to lower values of wiborgite crystallization temperatures from the Wiborg (670–890 °C) and Salmi (680–780 °C) rapakivi batholiths. To analyse pressure variations in rapakivi polybaric magmatic systems, more quartz grain measurements from different rapakivi granitic types have to be made.

Acknowledgements. This study was funded by the Estonian Science Foundation (grants Nos 7315 and 8963) and the Estonian Ministry of Education and Research (target research project No. SF0140016s09).

REFERENCES

Amelin, Y. V., Larin, A. M. & Robert, D. T. 1997. Chronology of multiphase emplacement of the Salmi rapakivi granite-anorthosite complex, Baltic Shield: implications for magmatic evolution. *Contributions to Mineralogy and Petrology*, **127**, 353–368.

Bachmann, O. 2010. The petrology evolution and pre-eruptive conditions of the rhyolitic Kos Plateau Tuff (Aegean arc). *Central European Journal of Geosciences*, **2**, 270–305.

Behr, W. M. & Platt, J. P. 2011. A naturally constrained stress profile through the middle crust in an extensional terrane. *Earth and Planetary Science Letters*, **303**, 181–192.

Eklund, O. & Shebanov, A. D. 1999. The origin of rapakivi texture by sub-isothermal decompression. *Precambrian Research*, **95**, 129–146.

Eklund, O. & Shebanov, A. 2005. Prolonged postcollisional shoshonitic magmatism in the southern Svecofennian domain – a case study of the Åva granite–lamprophyre ring complex. *Lithos*, **80**, 229–247.

Elliott, B. A. 2001. Crystallization conditions of the Wiborg rapakivi batholith, SE Finland: an evaluation of amphibole and biotite mineral chemistry. *Mineralogy and Petrology*, **72**, 305–324.

Flem, B., Larsen, R. B., Grimstvedt, A. & Mansfeld, J. 2002. In situ analysis of trace elements in quartz by using laser ablation inductively coupled plasma mass spectrometry. *Chemical Geology*, **182**, 237–247.

Girard, G. & Stix, J. 2010. Rapid extraction of discrete magma batches from a large differentiating magma chamber: the Central Plateau Member rhyolites, Yellowstone Caldera, Wyoming. *Contributions to Mineralogy and Petrology*, **160**, 441–465.

Götze, J., Plötze, M. & Habermann, D. 2001. Origin, spectral characteristics and practical applications of the cathodoluminescence (CL) of quartz – a review. *Mineral Petrology*, **71**, 225–250.

Götze, J., Plötze, M., Graupner, T., Hallbauer, D. K. & Bray, C. J. 2004. Trace element incorporation into quartz: a combined study by ICP-MS, electron spin resonance, cathodoluminescence, capillary ion analysis and gas chromatography. *Geochimica et Cosmochimica Acta*, **68**, 3741–3759.

Götze, J., Plötze, M. & Trautmann, T. 2005. Structure and luminescence characteristics of quartz from pegmatites. *American Mineralogist*, **90**, 13–21.

Holness, M. B. & Sawyer, E. 2008. On the pseudomorphing of melt-filled pores during the crystallization of magmatites. *Journal of Petrology*, **49**, 1343–1363.

Johnson, B. W., Bowman, J. R., Nash, B. P., Bartley, J. M. & Valley, J. W. 2009. TitaniQ, cathodluminescence and oxygen isotope analyses of the Alta stock, UT: geochemical insights into pluton assembly. *Geological Society of America, Abstracts with Programs*, **41**(7), 58.

Johnson, E. A., Sutherland, C., Logan, M. A. V., Samson, S. D. & Feely, M. 2011. Emplacement conditions of a porphyritic felsite dyke and timing of motion along the Coolin fault at Ben Levy, Co. Galway. *Irish Journal of Earth Sciences*, **29**, 1–13.

Kirs, J., Puura, V., Soesoo, A., Klein, V., Konsa, M., Koppelmaa, H., Niin, M. & Urtson, K. 2009. The crystalline basement of Estonia: rock complex of the Palaeoproterozoic Orosirian and Statherian and Mesoproterozoic Calymmian Periods, and regional correlations. *Estonian Journal of Earth Sciences*, **58**, 219–228.

Kohn, M. J. & Northrup, C. J. 2009. Taking mylonites' temperatures. *Geology*, **37**, 47–50.

Koistinen, T., Klein, V., Koppelmaa, H., Korsman, H., Lahtinen, R., Nironen, M., Puura, V., Saltykova, T., Tikhomirov, S. & Yanovskiy, A. 1996. Palaeoproterozoic Svecofennian orogenic belts in the surroundings of the Gulf of Finland. In *Explanation of the Map of Precambrian Basement of the Gulf of Finland and Surrounding Area 1 : 1 mill.* (Koistinen, T., ed.), pp. 21–57. Geological Survey of Finland, Special Paper 21.

Larsen, R. B., Polvé, M. & Juve, G. 2000. Granite pegmatite quartz from Evje-Iveland: trace element of high-purity quartz. *NGU Bulletin*, **436**, 57–65.

Larsen, R. B., Henderson, I., Ihlen, P. M. & Jacamon, F. 2004. Distribution and petrogenetic behaviour of trace elements in granitic pegmatite quartz from South Norway. *Contributions to Mineralogy and Petrology*, **147**, 615–628.

Lowers, H. A., Rusk, B. G. & Koenig, A. 2007. Application of the TitaniQ geothermometer to hydrothermal quartz. *Geological Society of America, Abstracts with Programs*, **39**(6), 607.

Mercer, C. M. & Reed, M. H. 2007. Insights into the formation of deep hydrothermal quartz from the porphyry-copper-molybdenum deposit at Butte, Montana. *American Geophysical Union*, abstract V41D-0816 [http://adsabs.harvard.edu//abs/2007AGUFM.V41D0816M, accessed 12 March 2012].

Müller, A., Wiedenbeck, M., Van Den Kerkhof, A. M., Kronz, A. & Simon, K. 2003a. Trace elements in quartz – a combined electron microprobe, secondary ion mass spectrometry, laser-ablation ICP-MS, and cathodluminescence study. *European Journal of Mineralogy*, **15**, 747–763.

Müller, A., Rene, M., Behr, H.-J. & Kronz, A. 2003b. Trace elements and cathodluminescence of igneous quartz in topaz granites from the Hub Stock (Slavkovsky Les Mts., Czech Republic). *Mineralogy and Petrology*, **79**, 167–191.

Müller, A., Seltmann, R., Kober, B., Eklund, O., Jeffries, T. & Kronz, A. 2008. Compositional zoning of rapakivi feldspars and coexisting quartz phenocrysts. *Canadian Mineralogist*, **46**, 1417–1442.

Nekvasil, H. 1991. Ascent of felsic magmas and formation of rapakivi. *American Mineralogist*, **76**, 1279–1290.

Nironen, M. 2006. Kansainvälinen ekskursio Suursaareen 12.–17.6.2005 [International Excursion to Suursaari 12.–17.06.2005]. *Geologi*, **58**, 23–31 [in Finnish].

Peterman, E. M. & Grove, M. 2010. Growth conditions of symplectic muscovite + quartz: implications for quantifying retrograde metamorphism in exhumed magmatic arcs. *Geology*, **38**, 1071–1074.

Putirka, K., Johnson, M., Kinzler, R., Longhi, J. & Walker, D. 1996. Thermobarometry of mafic igneous rocks based on clinopyroxene-liquid equilibria, 0–30 kbar. *Contributions to Mineralogy and Petrology*, **123**, 92–108.

Reid, M. R., Vazquez, J. A. & Schmitt, A. K. 2011. Zircone-scale insights into the history of a Supervolcano, Bishop Tuff, Long Valley, California, with implications for the Ti-in-zircon geothermometer. *Contributions to Mineralogy and Petrology*, **161**, 293–311.

Rämö, O. T. & Haapala, I. 1995. One hundred years of Rapakivi Granite. *Mineralogy and Petrology*, **52**, 129–185.

Rämö, O. T., Mänttari, I., Harju, S., Luttinen, A. V., Kohonen, J. & Heinonen, A. P. 2010. Supracrustal rocks associated with the Wiborg rapakivi granite batholith, southeastern Finland and vicinity. In *29th Nordic Geological Winter Meeting, Oslo, January 11–13, 2010. NGF Abstract and Proceedings of the Geological Society of Norway 1. Trondheim: Norsk Geologisk Förening*, pp. 167–168.

Shane, P., Smith, V. C. & Nairn, I. 2008. Millennial timescale resolution of rhyolite magma recharge at Tarawere volcano: insights from quartz chemistry and melt inclusions. *Contributions to Mineralogy and Petrology*, **156**, 397–411.

Shebanov, A. D., Belyaev, A. M. & Savatenkov, V. M. 1996. The significance of residual source material (restite) in rapakivi granite petrogenesis: an example from Salmi batholith, Russian Karelia. In *Symposium on Rapakivi Granites and Related Rocks* (Haapala, I., Rämö, O. T. & Kosunen, P., eds), p. 65. Helsinki, Finland.

Smith, V., Shane, P. & Nairn, I. 2010. Insights into silicic melt generation using plagioclase, quartz and melt inclusions from the caldera-forming Rotoiti eruption, Taupo volcanic zone, New Zealand. *Contributions to Mineralogy and Petrology*, **160**, 951–971.

Soesoo, A. 1993. Estonian porphyraceous potassium granites: petrochemical subdivision and petrogenetical interpretation.

Proceedings of the Estonian Academy of Sciences, Geology, **42**, 97–109.
Soesoo, A. 1997. A multivariate statistical analysis of clinopyroxene composition: empirical coordinates for the crystallisation PT-estimations. *GFF*, **119**, 55–60.
Soesoo, A. & Niin, M. 1992. Petrographical and petrochemical features of the Estonian porphyritic potassium granites. *Proceedings of the Estonian Academy of Sciences, Geology*, **41**, 93–107.
Soesoo, A. & Hade, S. 2010. A-type granitoids of Estonia. In *International Conference of A-Type Granites and Related Rocks Through Time, Abstract Volume, 18–20.08.2010; Helsinki* (Rämö, T., Lukkari, S. & Heinonen, A., eds), pp. 104–106. Helsinki University Press, Helsinki.
Soesoo, A., Puura, V., Kirs, J., Petersell, V., Niin, M. & All, T. 2004. Outlines of the Precambrian basement of Estonia. *Proceedings of the Estonian Academy of Sciences, Geology*, **53**, 149–164.
Spear, F. S. & Wark, D. A. 2009. Cathodoluminescence imaging and titanium thermometry in metamorphic quartz. *Journal of Metamorphic Geology*, **27**, 187–205.
Storm, L. C. & Spear, F. S. 2009. Application of the titanium-in-quartz thermometer to pelitic migmatites from the Adirondack Highlands, New York. *Journal of Metamorphic Geology*, **27**, 479–494.
Thomas, J. B., Watson, E. B., Spear, F. S., Shemella, P. T., Nayak, S. K. & Lanzirotti, A. 2010. TitaniQ under pressure: the effect of pressure and temperature on the solubility of Ti in quartz. *Contributions to Mineralogy and Petrology*, **160**, 743–759.
Vaasjoki, M., Rämö, O. T. & Sakko, M. 1991. New U-Pb ages from the Wiborg rapakivi area: constraints on the temporal evolution of the rapakivi granite-anorthosite-diabase dyke association of southeastern Finland. *Precambrian Research*, **51**, 227–243.
Väisänen, M., Mänttäri, I., Kriegsman, L. M. & Hölttä, P. 2000. Tectonic setting of post-collisional magmatism in the Palaeoproterozoic Svecofennian Orogen, SW Finland. *Lithos*, **54**, 63–81.
Wark, D. A. & Watson, E. B. 2006. TitaniQ: a titanium-in-quartz geothermometer. *Contributions to Mineralogy and Petrology*, **152**, 743–754.
Wark, D. A., Hildreth, W., Spear, F. S., Cherniak, D. J. & Watson, E. B. 2007. Pre-eruption recharge of the Bishop magma system. *Geology*, **35**, 235–238.
Watson, E. B. & Harrison, T. M. 1983. Zircon saturation revisited: temperature and composition effects in a variety of crustal magma types. *Earth and Planetary Science Letters*, **64**, 295–304.
Wiebe, R. A., Wark, D. A. & Hawkins, D. P. 2007. Insights from quartz cathodoluminescence zoning into crystallization of the Vinalhaven granite, coastal Maine. *Contributions to Mineralogy and Petrology*, **154**, 439–453.
Wilcock, J., Minarik, W. G., Goff, F. E. & Stix, J. 2009. Compositional and thermal zoning within quartz ejected before, during and after a supervolcanic eruption at 1.256 Ma: Valles Caldera, New Mexico, USA. *American Geophysical Union, Fall Meeting,* 2009, abstract V23C-2089 [http://adsabs.harvard.edu//abs/2009AGUFM.V23C2089W, accessed 28 May 2012].

Titaan-kvartsis geotermomeetria meetodi rakendamine paleoproterosoilise Suursaare kvartsporfüüri kristalliseerumistemperatuuride määramisel

Kairi Ehrlich, Evelin Verš, Juho Kirs ja Alvar Soesoo

Suursaare vulkaaniline kompleks kuulub Fennoskandia kilbi lõunaosas paiknevasse Viiburi rabakivigraniitsesse plutooni, mille intrusiivsed kivimid on kristalliseerunud rõhul 1–5 kilobaari ja temperatuuril 670–890 °C. Suursaare kvartsporfüürse laavakivimi kristalliseerumistemperatuuri hindamiseks analüüsiti Mäkiinpäällyse paljandist kogutud kivimiproovist fenokristallide ja põhimassi kvartsi induktiivseostatud plasmaemissiooni mass-spektromeetril laserablatsiooni meetodil. Kvartsi kristalliseerumistemperatuurid arvutati titaan-kvartsis geotermomeetria (TitaniQ) meetodil, mis seostab eksperimentaalselt gradueeritud kvartsi titaanisisalduse selle kristalliseerumistemperatuuriga titaanist küllastunud *fluid*'i-magmasüsteemis. Arvutustulemuste järgi jäävad Suursaare kvartsporfüüri kristalliseerumistemperatuurid vahemikku 647–738 °C. Uuring kinnitas Suursaare kvartsporfüüri kvartsi kahegeneratsioonilist, fenokristallide kõrgema- ja põhimassi terade madalamatemperatuurilist teket.